THE MAGNETIC EFFECTS OF BRECCIATION AND SHOCK IN METEORITES: II. THE UREILITES AND EVIDENCE FOR STRONG NEBULAR MAGNETIC FIELDS

AVIVA BRECHER

Dept. of Physics, Wellesley College, Wellesley, Mass., U.S.A. and Dept. of Earth and Planetary Sciences, Massachusetts Institute of Technology, Cambridge, Mass., U.S.A.

and

MIRIAM FUHRMAN

Dept. of Earth and Planetary Sciences, Massachusetts Institute of Technology, Cambridge, Mass., U.S.A.

(Received 7 August, 1978)

Abstract. We have examined the magnetic characteristics of representative ureilites, with a view to identify the magnetic effects of shock and to isolate a primary component of the natural remanent magnetization (NRM). As a group, the ureilites show remarkably uniform patterns of magnetic behavior, attesting to a common genesis and history. However, a clearly observed gradation in magnetic properties of the ureilites studied with shock level, parallels their classification based on petrologic and chemical fractionation shock-related trends.

The ureilite meteorites possess a strong and directionally stable NRM. Laboratory thermal modelling of this presumably primordial NRM preserved in Goalpara and Kenna produced reliable paleointensity estimates of order 1 Oe, thus providing evidence for strong early, nebular magnetic fields. This paleofield strength is compatible with values obtained previously from carbonaceous chondrites and supports isotopic evidence for a contemporary origin of these two groups of meteorites in the same nebular region. The mechanism for recording nebular fields, manifestly different in carbonaceous chondrite vs. ureilite meteorites, is thus relatively unimportant: violent collisional shock in ureilites seems to have only partially altered an original magnetization, by preferential removal of its least stable portion.

1. Introduction

The ureilite (U) achondrites are a unique class of meteorites whose peculiar chemical, mineralogical and petrologic characteristics are attributed to severe collisional shock in space (Vdovykin, 1970, 1976). They are considered by some to be analogous to terrestrial dunites, i.e., ultrabasic mantle-derived rocks (*ibid.*), which later underwent recrystallization and further reduction as a result of collisional impact shock (Wlotzka, 1972; Ramdohr, 1972; Marvin and Wood, 1972). Others maintain that the ureilites, rather than bearing evidence of planetary differentiation and evolution processes, are primitive meteorites, which are enriched in the high-temperature nebular early condensates, similar to those found in the carbonaceous C3V meteorites (Wänke *et al.*, 1972; Wiik, 1972). This latter view is supported by oxygen-isotopic evidence that these two groups (U and C) have originated in the same nebular neighborhood distinct from the region of formation of the Earth, Moon, and differentiated meteorite classes (Clayton *et al.*, 1976). Since the Ca–Al

The Moon and the Planets **20** (1979) 251–263. 0165–0807/79/0203–0251$01.95

rich inclusions of the Allende (C3V) carbonaceous chondrite, as determined by radio chronology, are among the earliest objects dated in the solar system (e.g., Wetherill, 1975), the ureilites may have preserved not only chemical, but also magnetic information pertaining to the nebular and protoplanetary formative stages. Alternatively, at a later date, if the collisional shock which modified so drastically their mineralogy, disturbed or totally reset their magnetic minerals, the thermal event associated with shock should have enabled them to record the ambient magnetic field at post-shock cooling. In fact, the morphology and implied shock-reduction generation of a nearly pure Fe metal component in ureilites are strikingly analogous to those encountered in lunar breccias and poikilitic (impact-melt) rocks. Therefore, comparative magnetic studies of lunar and ureilite rocks, which contain Ni–Fe–Co magnetic metal carriers of similar composition and amounts hold promise in identifying and calibrating the thermomagnetic effects of collisional shock cratering (Brecher and Stein, 1975; Brecher, 1976b) in the broader, planetary context.

Finally, a recent analysis of the Kenna ureilite (Berkeley, *et al.*, 1976) ascribed a pronounced cumulate fabric to early igneous and later mild metamorphic processes on the parent body, followed by fracturing and deformation induced by 50–250 kbar shock. In contrast, Goalpara shows evidence of extensive recrystallization and annealing associated with severe shock (~ 600 kb) (Carter *et al.*, 1968). A continuous spectrum of compositional fractionation in siderophiles and other chemical elements in ureilites was observed by Wasson *et al.* (1976), which led to an ordering of ureilites as a suite of decreasing shock level and increasing depth of origin in the parent asteroidal body in the following sequence: Goalpara, Haverö, Dyalpur, Novo-Urei, Kenna. A magnetic characterization of typical ureilites across the spectrum would provide an independent verification of this classification in terms of shock effects and clarify the extent to which primary textures and minerals still dominate or survive shock-modification (e.g., Berkeley *et al.*, 1976).

2. Meteorite Samples and Initial Magnetic Measurements

Samples of three representative and well-studied ureilites, across the shock, textural and chemical spectrum were obtained from Drs C. Frondel (Harvard collection), C. Allègre and L. Wilkening. From examinations under a petrographic microscope, our samples appear to conform to literature petrographic descriptions. Larger samples (Kenna and Goalpara, Table I), were cut into two subsamples (a, b), preserving their mutual orientation for magnetic measurements, to test the small-scale magnetic homogeneity (Figure 1, Table I). The larger-scale uniformity could also be assessed for Kenna, where two different specimens from the strewn field were available; and for Haverö, from a comparison with magnetic data published by Neuvonen *et al.* (1972). Some magnetic data on Novo-Urei are also available (Larson *et al.*, 1973; Guskova, 1972) and are included in Table I, where the meteorites are listed in order of decreasing shock metamorphism.

Initial magnetic measurements consist of bulk magnetic susceptibility (χ) and natural magnetic remanence (NRM) intensity (Table I).

The bulk susceptibilities were measured with a Bison 3101 system, with a dynamic

TABLE I

Magnetic properties of ureilites

		Volume (cm^3)	NRM ($emu\ cm^{-3}$)	χ ($\times 10^{-3}$) ($G\ cm^{-3}\ Oe^{-1}$)	$Q = \frac{NRM}{\chi 1\ Oe}$	IRM_S ($emu\ cm^{-3}$)	$\frac{IRM_S}{NRM}$	Paleofield estimate	Refs.
Goalpara	(a)	1.67	3.53×10^{-2}	135	0.3	3.08	87	1.4 Oe	[1]
	(b)	1.51	4×10^{-2}	115	0.3			0.4 Oe	[1]
			3×10^{-2} emu/g						[3]
Haverö		0.06	5.43×10^{-1}	72	8	9.29×10^{-1}	1.71		[1]
			0.15×10^{-1}	28	1				[2]
Novo Urei			1.5×10^{-3} emu/g						[3]
			1.6×10^{-3}	20	0.08				[4]
Kenna	1(a)	0.47	8.25×10^{-1}	24.8	33	2.61	3.16	0.86 Oe	[1]
	1(b)	0.09	8.38×10^{-1}	23.6	36	2.42	2.9		[1]
	2.	0.06	8.73×10^{-1}	10.6	82	6.43	7.37		[1]

Explanatory Note: a and b are oriented pairs.

References: [1] This work; [2] Neuvonen *et al.* (1972); [3] Larson *et al.* (1973); [4] Guskova (1972).

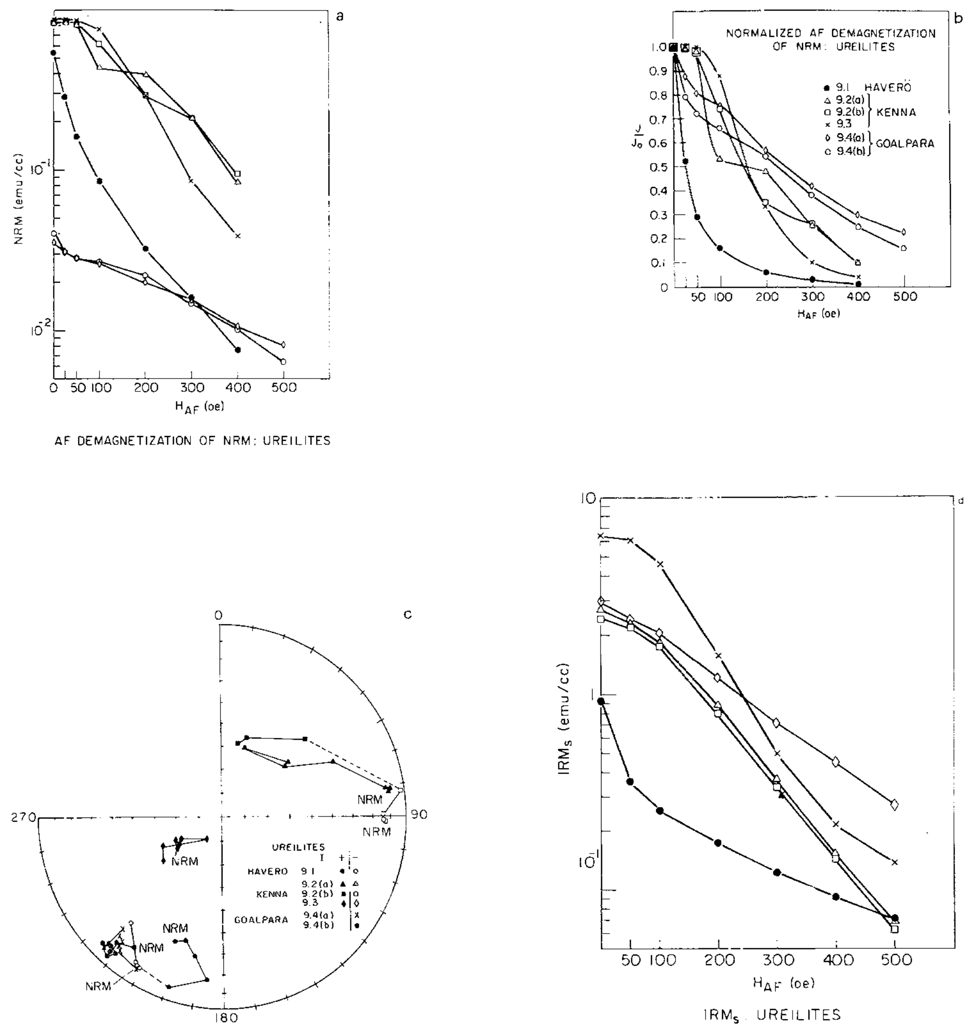

Figs. 1a–1d. The ureilites have an unusually strong and stable natural remanent magnetization (NRM). NRM intensity is in the range 0.01–1 emu cm^{-3} (1a). Stability of NRM intensity to stepwise AF demagnetization (peak field, H_{AF} in Oersted) is shown on an absolute scale (1a) and normalized to NRM value (1b). Relative (arbitrary) NRM directions are plotted in projection on a stereonet (1c): Note the tight directional clustering for Goalpara (a, b) and Kenna samples and parallel directional convergence in the Kenna (a, b) oriented subsamples. This type of hard coercivity spectra and directional convergence under AF cleaning indicate that NRM is probably a true paleoremanence. The saturation remanence (IRM_S) intensities and demagnetization spectra (1d) are shown on an absolute magnitude scale vs. peak cleaning field (H_{AF}) using the same symbol code as in Figures 1(a) and 1(b).

range of 10^{-6} to 10^{-1} G Oe^{-1} cm^{-3} in 0.5 Oe applied field. The values, which give a rough measure of metal abundance – assuming similar grain-size distribution – cluster in a narrow range over the 10^{-2} to 10^{-1} emu decade. The magnetic susceptibility increases with shock (from 10–25 x 10^{-3} emu for Kenna to 120 x 10^{-3} for Goalpara), in accord with the addition of shock-reduced metal, with increasing shock level, to the primary metal fraction. These comparatively high values for stony meteorites (e.g., Brecher and Ranganayaki, 1975; Brecher *et al.*, 1977) are consistent with the inferred enrichment of ureilites in shock-generated metal up to ~ 6 wt.%. The published data on metal contents (wt.%) in ureilites are as follows: North Haig, 0.34; Dingo Pup Donga, 3.07; Goalpara, 5.86; Haverö, 3.6–6, roughly in order of increasing shock (cf. Vdovykin, 1970, 1976; Jedwab, 1972; Marvin and Wood, 1972; Neuvonen *et al.*, 1972; Ramdohr, 1972; Wlotzka, 1972). The concentration, composition and morphology of metal is highly variable within each meteorite, a fact which is indicative of highly localized effects of shock. Indeed, in Haverö Ni-poor ($\lesssim$ 1% Ni–Fe) metal in olivine is ascribed to an origin by shock-reduction *in situ*, whereas primary metal in veins, fractures, and blebs, possibly remelted and redistributed by shock-heating, is higher in Ni (~ 3%) (e.g., Wlotzka, 1972). The metal occurs mainly as strongly magnetic kamacite (e.g., Neuvonen *et al.*, 1972; Ramdohr, 1972), often with strong vein-lineation, when filling oriented arrays of fractures (e.g., Berkeley *et al.*, 1976, in Kenna) or with preferred crystallographic orientation and tabular morphology (e.g., Ramdohr, 1972, in Haverö). The metal grain size spectrum is also unusually broad (e.g., Wlotzka, 1972, in Haverö). These factors contribute to the observed high NRM intensity (Table I, Figure 1) and its stability behavior (Section 3).

The NRM values are also relatively high, contained in a rather narrow range of two orders of magnitude ($\sim 3 \times 10^{-2}$ 9×10^{-1}), (Figure 1, Table I). As a group the ureilites are more intensely and more homogeneously magnetized than other stony meteorites, except for the carbonaceous chondrites (Brecher and Ranganayaki, 1975; Brecher and Arrhenius, 1974; Brecher, 1972, 1977b, c).

The intensity of NRM is inversely correlated with shock, attesting to partial shock demagnetization. This effect was also observed in both lunar and terrestrial shocked rocks (Brecher *et al.*, 1975b; Cisowski *et al.*, 1976): Goalpara, the most heavily shocked (to ~ 600 kb, Vdovykin, 1970) has the lowest NRM intensity; Haverö, which shows intermediate shock symptoms (Wasson *et al.*, 1976), has the next highest NRM; Kenna at the low shock extreme (50–250 kbar), but with the most pronounced oriented petrofabric (Berkeley *et al.*, 1976; Wasson *et al.*, 1976) has the strongest NRM.

The Koenigsberger ratios, $Q = \text{NRM}/\chi \cdot H$, of remanent to induced magnetization, also ranges over two decades, from 0.08 to 80 – parallel to NRM values, increasing with decreasing shock, as NRM is lower, but χ is higher at the high-shock level. Q measures the relative importance of remanent vs. induced moments: if $Q > 1$, fine-grained carriers of probably stable NRM dominate; for $0.1 \lesssim Q < 1$, coarse, multi-domain magnetic grains influence remanent behavior.

3. Demagnetization Behavior of NRM and IRM_s

Samples of three ureilites (Table I) were progressively demagnetized in alternating fields (AF) up to 500 Oe peak values (Figure 1). The experimental apparatus and procedure are described in Brecher and Ranganayaki (1975). The resulting coercivity spectra (Figure 1a, b) are indicative of the stability of the original magnetization to viscous relaxation and magnetic resetting. Two mutually oriented subsamples of each Goalpara and Kenna (a, b) and a third individual hand specimen of Kenna show closely similar NRM intensity and coercivity spectra (Figure 1a, b), indicating that the amounts and grain sizes of metal are quite homogeneously distributed and rather uniformly magnetized, within each meteorite.

The relative NRM stability gradation with shock is not as clear-cut as for the NRM level (Figure 1b). The highly shocked Goalpara has indeed the hardest, and therefore most stable NRM demagnetization curve, but Haverö, though intermediate on the shock scale, has the softest coercivity spectrum. Kenna has a higher coercivity of NRM in the low fields range ($\lesssim 100$ Oe) and relatively softer spectrum for $H_{AF} > 100$ Oe.

The corresponding directional changes in stepwise AF demagnetization of NRM are plotted in stereographic projection in Figure 1(c). Better directional coherence seems to be associated with higher shock: the NRM vector is directionally stable in Goalpara; it migrates moderately in Haverö and considerably in Kenna (Figures 1(a, b)). Higher resolution plots of magnetization vectors projected on two orthogonal planes (as shown in Figure 3(c)) suggest that only a single-component, hard NRM is preserved in Goalpara; a two-component NRM, with a large soft contribution, is found in Haverö. Kenna (1a, b) samples have a multi-phase remanence with three directionally distinct components, the largest being of low to intermediate coercivity ($50 < H_{AF} \lesssim 200$ Oe), and a stable, hard, but weaker high-coercivity residual (200–500 Oe). There is, however, some internal variability in NRM hardness and directional stability among Kenna specimens (Figure 1(a–c)).

The saturation remanence (IRM_s) values imparted in 10 kOe fields are only a factor of a few (x 1–10) larger than those of natural remanence (Table I), so that the ureilites were magnetized close to their saturation capacity; in contrast, other achondrite groups are severely undersaturated (Brecher and Stein, 1975). The extreme case is Goalpara, whose soft NRM portion was evidently shock-demagnetized, thus effectively raising the IRM_s/NRM ratio (Table I).

The AF demagnetization stability characteristics of IRM_s (Figure 1(d)) closely parallel those of NRM (Figure 1(a, b)): Goalpara has, relatively, the hardest and Haverö the softest coercivity spectrum. This order of relative stability does not match the order of decreasing severity of shock (Table I). At intermediate shock (Haverö), thermal anneal effects effectively counterbalance shock-hardening effects, whereas at highest shock (Goalpara), the newly added shock-reduced, finely disseminated metal grains contribute to the increase in magnetic coercivity. At lowest shock (Kenna), the shock hardening may be due only to removal of a soft NRM component residing in coarse grains. Thus, a gradation in IRM_s intensity and stability corresponding to that in shock level is evident only in the high-coercivity ($\gtrsim 200$ Oe) portion of the normalized AF demagnetization curves.

All magnetic observations discussed above can be interpreted in the framework of NRM demagnetization and hardening by a shock event, which modified the original remanence by preferentially removing – to various degrees – its low-coercivity portion.

4. Determination of Fossil Magnetic Field-Strength

A most desirable and significant result of these magnetic studies is to determine an approximate 'fossil' magnetic field intensity, in which the component of NRM isolated and identified as 'primeval' was imparted. Such a paleointensity determination, if reliable, underscores the importance of magnetic studies for constraining models of genesis of ureilites and their physical environment. Although shock and brecciation commonly introduce complex features of magnetic behavior associated with cold fracturing and post-shock thermal metamorphism (e.g., Brecher and Ranganayaki, 1975; Brecher *et al.*, 1977), in the ureilites they are gradual and relatively simple, a fact which argues in favor of a unique collisional shock-event involving a single parent body (Wasson, *et al.*, 1976). In Goalpara, Figure 2(c) shows evidence that a stable, single-component, unidirectional NRM has survived disturbance by shock. Because of the gradation in magnetic properties with shock discussed above, it is unlikely, though possible, that this NRM was introduced by shock or at post-shock cooling.

However, there is a remarkably close similarity in both intensity and coercivity spectrum of the NRM ($\sim 3 \times 10^{-2}$ emu cm^{-3}) to repeat laboratory thermo-remanences acquired in fields of 1.4 Oe ($TRM_1^e \simeq 1.8 \times 10^{-2}$ emu cm^{-3}) and in 0.4 Oe ($TRM_2^e \simeq 4.4 \times 10^{-2}$ emu cm^{-3}), by heating and cooling from 800 °C to room temperature. It was seen that Goalpara is capable of acquiring a directionally stable and magnetically hard TRM, on the time scale of laboratory cooling comparable to the short times envisaged for post-shock cooling. This capability can be contrasted to the inability of lunar rocks and breccias to fix laboratory TRM (e.g., Brecher *et al.*, 1974). A comparison of the coercivity spectra of saturation remanence before (IRM_s) and after (IRM_s^2) heating in air to 800 °C, shows that any thermal alteration of magnetic grains was negligible (Figure 2(a, b)). Thus, a paleofield determination by the method successfully employed previously for carbonaceous (Brecher, 1972) and ordinary chondrites (Brecher and Ranganayaki, 1975; Brecher *et al.*, 1977) is fully justified. A best fit slope of 1.04 obtained from a regression plot of NRM loss vs. TRM loss in stepwise AF cleaning (Figure 2(d)) yielded a paleofield value of 1.4 Oe. This initial determination was followed by a second heating to above the Curie point of iron (770 °C) and cooling in zero-field, to check if a sizable spontaneous magnetization whose intensity and direction is texturally controlled occurs in this heavily foliated ureilite; the existence of such zero-field moments has been shown to invalidate paleofield intensity determinations on iron meteorites (Brecher and Albright, 1977), lunar rocks (e.g., Brecher, 1976b, 1977b) and even some shocked and metamorphosed ordinary chondrites (Brecher and Leung, 1978). The resulting spontaneous moment ($TRM_0 \sim 1 \times 10^{-3}$) is a factor of 30 lower than the NRM and $\times$ 20–40 below the two laboratory TRM moments. Figure 3 contrasts the jagged, irregular AF demagnetization curve of spontaneous magnetization and its directional scatter in the foliation plane, to the extremely well-behaved NRM and TRM. Such jagged and unstable moments are typical of the NRM in both lunar rocks (Brecher, 1976a) and brecciated achondrites (Brecher and Stein, 1975; Brecher, 1977a) and would disqualify a sample for paleointensity determinations. In Goalpara, however, the magnetic field prevails over textural

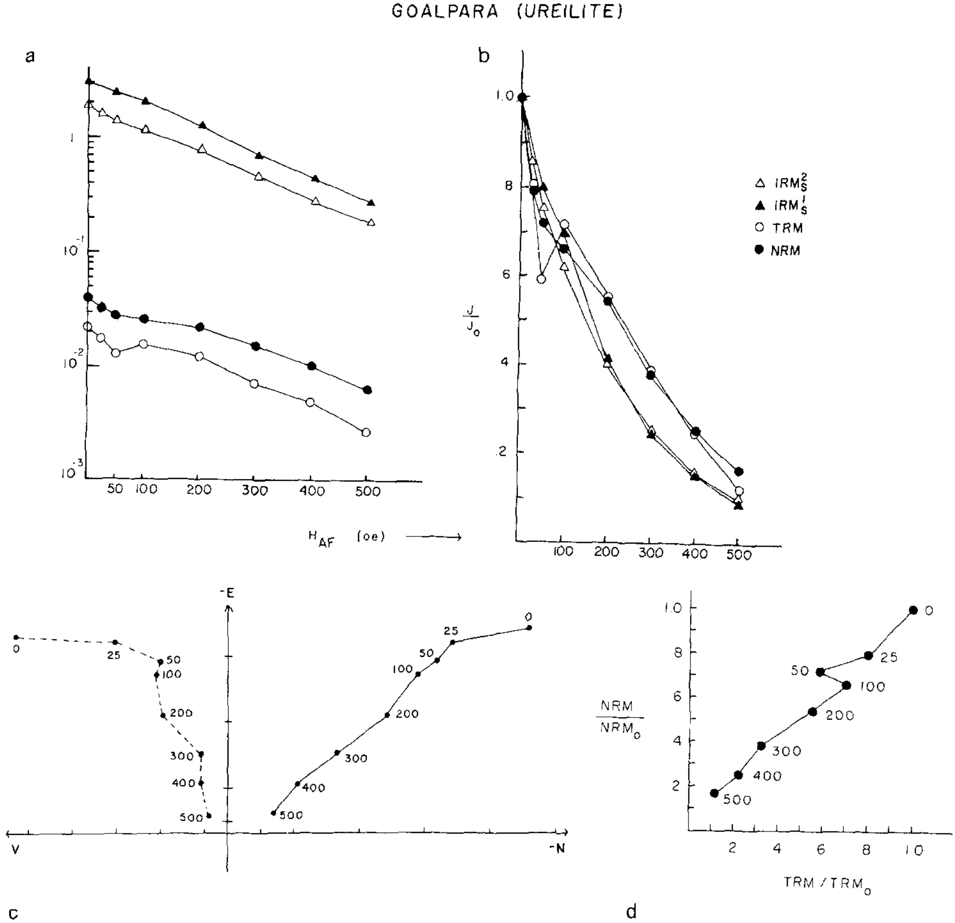

Figs. 2a–d. Determination of paleofield strength in Goalpara: The absolute (2a) and normalized (2b) AF coercivity spectra of NRM are compared to those of a laboratory TRM, following heating to 800 °C and cooling in the laboratory field. Shown also are the coercivity spectra of saturation remanence before (IRM_s^1) and after (IRM_s^2) heating; their close similarity points to negligible thermal alteration of magnetic grains.

(2c) A vector-diagram of the progressive AF demagnetization of NRM in Goalpara: directional changes are projected on two orthogonal (arbitrary) planes. Although there is a directionally distinct soft component, apparently removed in 25–50 Oe, the NRM consists mainly of a single unidirectional magnetization, stable up to 500 Oe.

(2d) A linear regression plot of the NRM vs. TRM residual at each step in the AF demagnetization process yields a best-fit slope of 1.04 and a paleofield estimate of 1.4 Oe, assuming that the proportionality $H_{anc}/H_{lab} \simeq$ NRM/TRM is obeyed.

control, and the direction of TRM follows the ambient field as well (Figure 3). A third heating followed by TRM_e^2 acquisition again closely reproduced the NRM intensity and demagnetization characteristics, reinforcing the inference that the NRM is of thermal origin, imprinted in an ambient magnetic field of comparable strength (of 0.4 Oe for TRM_e^2). Hence, an ancient field of order ~ 1 Oe is confidently estimated for Goalpara.

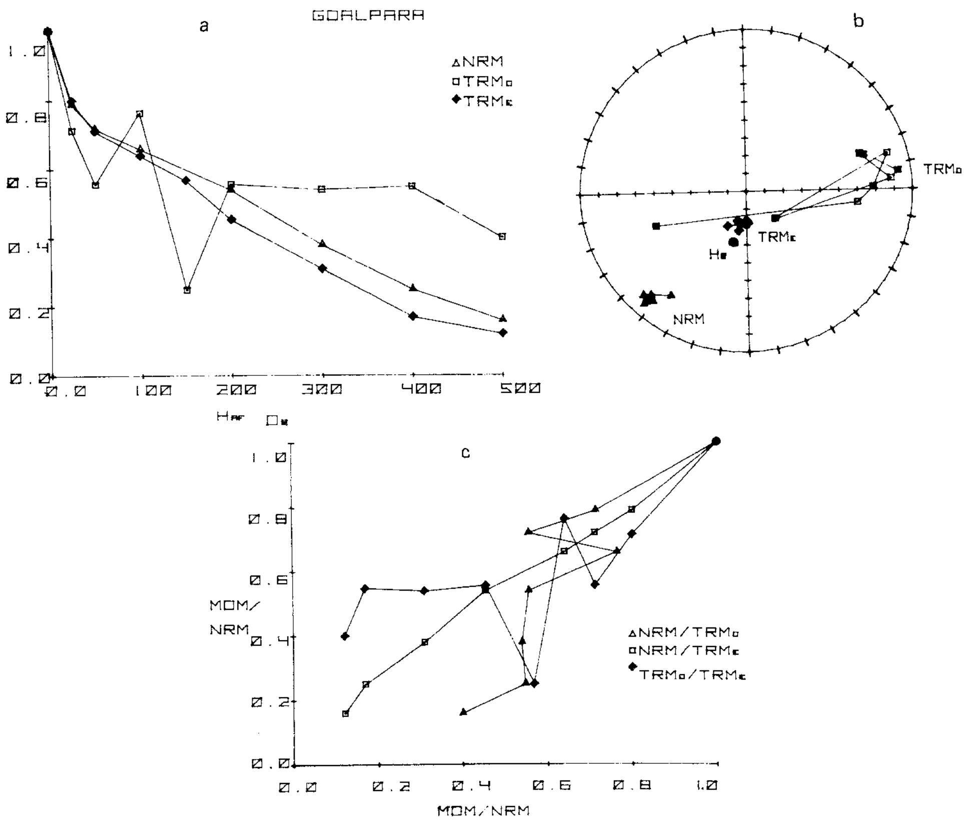

Figs. 3a–c. This is a repeat heating experiment for paleointensity determination on Goalpara:

(3a) contrast the irregular, jagged AF cleaning intensity profile of spontaneous magnetization (TRM_0), following zero-field cooling with that of TRM_e acquired at cooling from 800 °C in a laboratory field of 0.4 Oe. The latter is closely analogous to the NRM profile.

(3b) shows the directional clustering of both NRM and TRM vectors in AF cleaning, in contrast to scatter and reversal evident for the weaker TRM. The TRM_e direction coincides that of the ambient field (H_e).

(3c) is comparable to Figure 2(c), and shows that only the TRM/NRM residuals yield a linear plot of slope ~ 1 suitable for estimating a paleointensity. The TRM_0, which is an expression of shock-induced preferred-orientation of magnetic and petrographic fabric, does not mimic the behavior of a true TRM.

A Kenna specimen with a convergent, stable and unidirectional NRM (Figure 1) was also subjected to the above procedure for paleointensity determination (Figure 4), yielding an average field value of 0.86 Oe. Its NRM (8.73×10^{-1} emu cm^{-3}) was stronger, but softer than a thermoremanence ($TRM_e \simeq 2.1 \times 10^{-2}$ emu cm^{-3}) imprinted by cooling in a 0.4 Oe laboratory field (Figure 4): 75% of TRM_e survived cleaning in 300 Oe fields compared with only 10% for NRM. It thus appears that neither shock demagnetisation, nor shock hardening are important at low levels of shock. The best fit linear slope of NRM vs. TRM_e is steeper than in Goalpara, due perhaps to the negligible degree of shock demag-

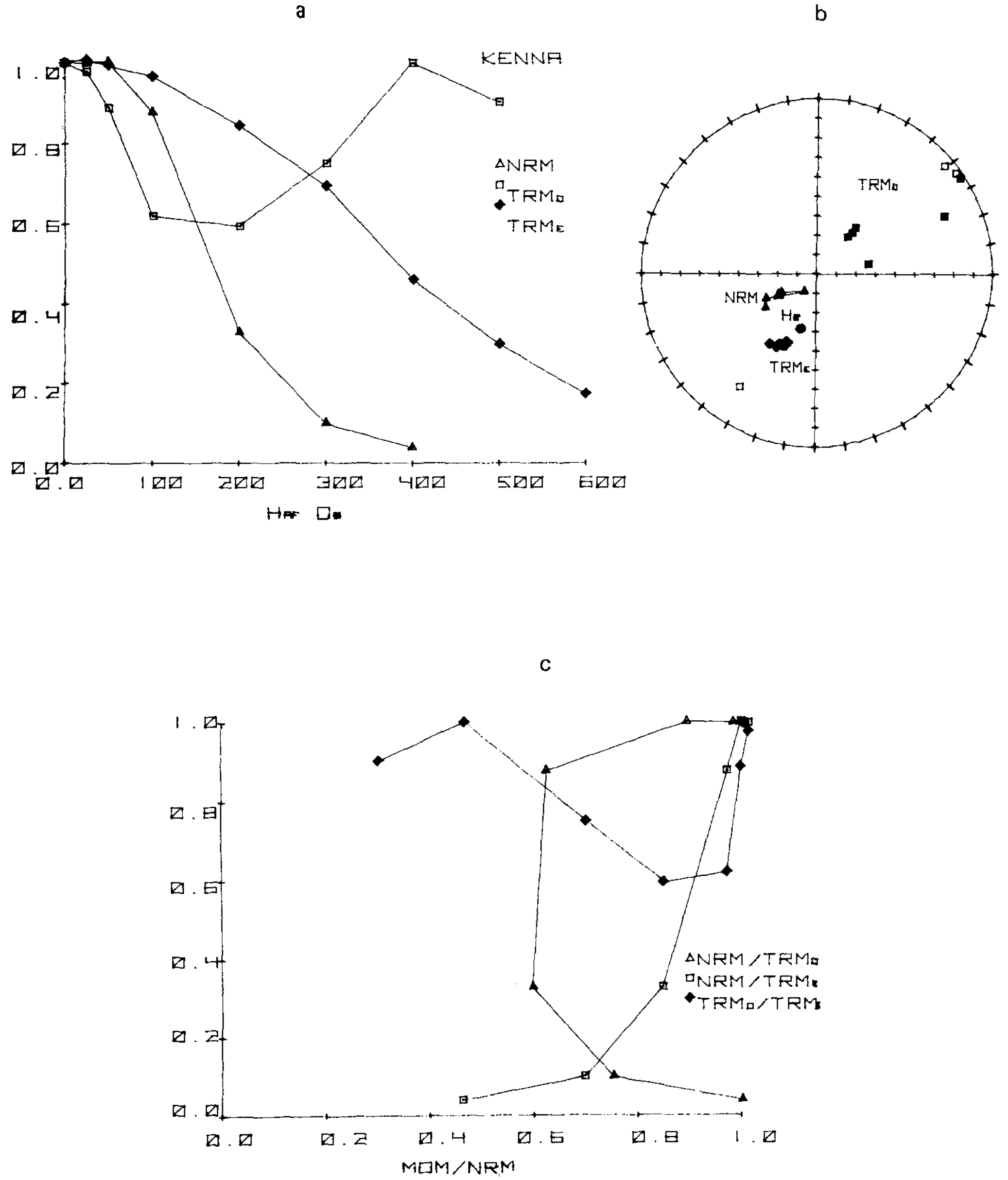

Figs. 4a–c. Figure 4 is similar to Figure 3, for the ureilite Kenna. The relative stability to AF demagnetization of NRM, spontaneous (TRM_0) and thermoremanent (TRM_e) moments are compared in Figure 4(a); their directional behavior is shown in Figure 4(b); and the paleointensity is derived from the best linear fit of NRM vs. TRM_e residuals in Figure 4(c). Again, TRM_0 is undemagnetizable, shows planar pinning to the preferred petrofabric plane in which NRM is found as well. TRM_e is harder than the NRM, but shows excellent directional coherence, being aligned with the lab field at cooling. The average paleointensity derived for Kenna is 0.86 Oe, assuming that its NRM is also of thermal nature.

netization. The excellent preservation of primary features in Kenna (Berkeley, *et al.*, 1976) is thus supported by magnetic evidence. Moreover, TRM_0 bears evidence of strong textural alignment of magnetic grains (Figure 4): though very weak (2.7×10^{-4} emu cm^{-3}), the zero-field moment is magnetically hard (Figure 4(a)) and strongly pinned to the oriented fabric plane, to which the NRM is also confined (Figure 4(b)). As the erratic NRM/TRM_0 curves show, the spontaneous magnetization cannot account for the NRM, whereas a ~ 1 Oe primary thermoremanence is an adequate analog.

5. Discussion

The paleofield strengths obtained from Goalpara and Kenna seem reliable and internally consistent by the stringent criteria for selecting meteorites with stable fossil NRM and for reproducing in the laboratory the observed NRM behavior.

The field values, of roughly 1 Oe, are close to ancient fields retrieved from carbonaceous chondrites by a variety of low-temperature methods (e.g., Brecher, 1977(c)). It is curious, though – we argue – not fortuitous, that similar ancient fields are indicated by the two classes of meteorites, whose enormously different thermal and shock histories place them at opposite ends of a thermal alteration spectrum. Based on magnetic characteristics, both classes are relatively coherent groups with fine intra-group gradations corresponding to chemical-petrological or shock-exposure differences. Both groups of meteorites are distinguished by unexpectedly homogeneous, strong, stable and directionally clustered NRM, indicative of a unique original magnetizing event, only modestly modified subsequently (e.g., Brecher, 1977a).

These magnetic results support the inference that both ureilites and carbonaceous chondrites have formed from related nebular material (e.g., Clayton and Mayeda, 1975; Clayton *et al.*, 1976) and provide further evidence for a strong external magnetic field present during the accretional stages and throughout an early bombardment stage (Wetherill, 1975) which possibly affected the ureilites. Other indirect evidence for strong extended solar magnetic fields has been reviewed by Sonett and Herbert (1977) in the context of asteroidal heating (see also Brecher *et al.*, 1975). It is unlikely that such magnetic fields were generated by shock (e.g., Meadows, 1972) or enhanced by shock, since: (a) Totally unshocked meteorites, such as carbonaceous chondrites, have recorded the same field intensities by clearly different, low-temperature magnetization mechanisms; hence the nature of the process of NRM acquisition is relatively unimportant, and (b) Both shocked and unshocked ordinary chondrites yield similar, systematically lower (0.01–0.1 Oe) paleofield values, with no evidence of a field strength correlation with shock level (Brecher, 1977a; Brecher and Ranganayaki, 1975; Brecher *et al.*, 1977a, b). This conclusion is very important in the ongoing debate regarding the nature of lunar magnetism and the relative importance of planetary surface processes. There is now convincing evidence from lunar rocks and terrestrial and meteoritic analogs that shock does not totally obliterate the useful paleoremanence, but predictably alters it (e.g., Cisowski *et al.*, 1976; Brecher *et al.*, 1975b). The gradation of magnetic properties with shock intensity among ureilites and among ordinary chondrites (Brecher *et al.*, 1977b) also argues in favor of this conclusion. We noted that for ureilites: (1) The magnetic susceptibility increases with severity of shock; and (2) The NRM intensity decreases, yet its coercivity spectrum generally hardens with increasing shock. Partial shock-demagnetization and removal of soft NRM components and the competing thermal effect of grain-growth may be responsible for these features. (3) The directional stability of NRM also improves with higher shock, reflecting the shock-hardening effect, and weakening the importance of primary oriented fabric in accounting for the magnetic behavior (e.g., Brecher, 1976, 1977). (4) The relative stability of saturation remanence (IRM_s) also correlates directly with shock level. (5) Magnetic parameters (Q, IRM_s/NRM) also vary systematically with shock level (Table I). In contrast to lunar rocks (e.g., Brecher *et al.*, 1974), the ureilites are quite capable of fixing a stable TRM in a laboratory field in cooling from above the Curie point of metal. Moreover, spontaneous magnetization associated with zero-field cooling is very unstable and much weaker than both NRM and TRM for Goalpara and Kenna (see Section 2 above) so that the demonstrated importance of oriented petrofabric for lunar rock magnetism (e.g., Brecher, 1976a, 1976d, 1977b) and for some classes of meteorites (e.g., Brecher and Albright, 1977; Brecher, Fuhrman and Leung, 1978, in preparation) is not relevant for ureilites, in spite of pronounced shock-metamorphic and primary oriented petrofabric and crystallographically-oriented metal phases (e.g., Berkeley, *et al.*, 1976; Vdovykin, 1970, 1976). Textural pinning of magnetization evident in the migration of NRM vector with progressive AF cleaning (see the stereonet plot of Figure 1(c)) in the preferred fabric plane is evident in Kenna, the ureilite with lowest shock exposure and strongest primary cumulate fabric (Berkeley *et al.*, 1976) and erased in Goalpara, where shock recrystallization and annealing apparently dominates due to removal of the soft magnetization residing in the largest metallic grains which conform to the original oriented fabric.

In the case of ureilites the thermal origin of a primary magnetization can be demonstrated experimentally and the magnitude of the magnetizing field can be estimated with confidence at ~ 1 Oe.

Acknowledgments

We thank Dr Olsen of the Chicago Field Museum, Professor Wänke of the University of Meinz and Professor Wilkening of the University of Arizona for kindly loaning meteorite samples. Ms Leung of Wellesley College is thanked for performing field-determination experiments. Ms Ikehara kindly typed this manuscript. We acknowledge support by NASA Grant NSG 9057 to Aviva Brecher and UROP-MIT sponsorship of Miriam Fuhrman.

References

Berkeley, J. L., Brown IV, H. G., Keil, K., Carter, N. L., Mercier, J. C., and Huss, G.: 1976, *Geochim. Cosmochim. Acta* **40**, 1429.

Brecher, A.: 1972, *Proc. CNRS Symp. on the Origin of the Solar System*, p. 260.
Brecher, A. and Arrhenius, G.: 1974, *J. Geophys. Res.* **79**, 2081.
Brecher, A., Menke, W. H., and Morash, K. R.: 1974, *Proc. 5th Lunar Sci. Conf.* Vol. 3, pp. 2795–2814.
Brecher, A. and Stein, J.: 1975, *EOS Trans. AGU* **56**, 1016.
Brecher, A. and Ranganayaki, R. P.: 1975, *Earth Planet. Sci. Letters* **25**, 57.
Brecher, A., Briggs, P. L., and Simmons, G.: 1975a, *Earth Planet. Sci. Letters* **28**, 37.
Brecher, A., Klonowski, M., and Simmons, G.: 1975b, *Lunar Science VI*, p. 80.
Brecher, A.: 1976a, *Earth Planet. Sci. Letters* **29**, 131.
Brecher, A.: 1976b, *Lunar Science VII*, p. 91.
Brecher, A.: 1976c, *Proc. Lunar Sci. Conf. 7th*, p. 2217.
Brecher, A.: 1977a, *Proc. Lunar Sci. Conf. 8th*, p. 703.
Brecher, A.: 1977b, in A. H. Delsemme (ed.), *Comets, Asteroids, Meteorites: Interrelations, Evolution and Origins*, Univ. of Toledo, p. 415.
Brecher, A.: 1977c, *Nature* **266**, 381.
Brecher, A. and Albright, L.: 1977, *J. Geomag. Geoelec.* **29**, 379.
Brecher, A., Fuhrman, M., and Albright, L.: 1977a, *Meteoritics* **12**, 185.
Brecher, A., Stein, J., and Fuhrman, M.: 1977b, *The Moon* **17**, 205.
Brecher, A. and Leung, L.: 1978, Abstract to be presented at Met. Soc. Meeting, Sudbury, Ontario, Canada.
Carter, N. L., Raleigh, C. B., and DeCarli, P.: 1968, *J. Geophys. Res.* **73**, 5439.
Cisowski, S. M., Fuller, M., and Wu, Y.: 1976, *Lunar Sci. VII*, p. 154.
Cisowski, S. M., Dunn, J. R., Fuller, M., Rose, M. F., and Wu, Y. M.: 1976, *Proc. Lunar Sci. Conf. 7th*, p. 3299.
Clayton, R. N., Mayeda, T. K., Onuma, N., and Shearer, J.: 1976, *Geochim. Cosmochim. Acta* **40**, 1475.
Guskova, Ye, G.: 1972, *The Magnetic Properties of Meteorites*, Nauka Press, Leningrad (108 pp.) and NASA Technical Transl. NASA-TT-F-792.
Jedwab, J.: 1972, *Meteoritics* **7**, 537.
Larson, E. E., Watson, D. E., Herndon, J. M., and Rowe, M. W.: 1973, *J. Geomag. Geoelec.* **25**, 331.
Marvin, U. B. and Wood, J. A.: 1972, *Meteoritics* **7**, 601.
Meadows, A. J.: 1972, *Nature* **237**, 274.
Neuvonen, K. J., Ohlson, B., Papunen, H., Häkli, T. A., and Ramdohr, P.: 1972, *Meteoritics* **7**, 515.
Ramdohr, P.: 1972, *Meteoritics* **7**, 565.
Sonett, C. P. and Herbert, F. L.: 1977, in A. H. Delsemme (ed.), *Comets, Asteroids, Meteorites: Interrelations, Evolution and Origins*, Univ. of Toledo, p. 429.
Vdovykin, G. P.: 1970, *Space Sci. Rev.* **10**, 483.
Vdovykin, G. P.: 1976, *Space Sci. Rev.* **18**, 749.
Wänke, H., Baddenhausen, H., Spettel, B., Teschke, F., Quijano-Rico. M., Dreibus, G., and Palme, H.: 1972, *Meteoritics* **7**, 579.
Wasson, J. T., Chou, C. L., Bild, R. W., and Baedecker. P. A.: 1976, *Geochim. Cosmochim. Acta* **40** 1449.
Wetherill, G. W.: 1975, *Ann. Rev. Nuclear Sci.* **25**, 283.
Wiik, H. B.: 1972, *Meteoritics* **7**, 553.
Wlotzka, F.: 1972, *Meteoritics* **7**, 591.